

Ca_{1-x}Na_{2x}Al₂B₂O₇: A Structure with Tunable Density of Na⁺ Vacancies

Meng He,* Hiroki Okudera, and Arndt Simon

Max Planck Institute for Solid State Research, Heisenbergstrasse 1, D-70569 Stuttgart, Germany

Received January 19, 2005

A series of samples with the composition Ca_{1-x}Na_{2x}Al₂B₂O₇ (0 < x ≤ 1) was investigated and a hexagonal structure with unusually large range of homogeneity (at least from x = 0.01 to 0.95) was revealed. The hexagonal phase consists of [Al₂B₂O₇]_∞²⁻ lamellae stacked along the *c* axis, as in CaAl₂B₂O₇ and Na₂Al₂B₂O₇. Nevertheless, the configuration and stacking sequence of the [Al₂B₂O₇]_∞²⁻ lamellae are different in these three structures. In the hexagonal structure of Ca_{1-x}Na_{2x}Al₂B₂O₇, Ca and half Na cations (Na1) statistically occupy the same crystallographic site which is located between the [Al₂B₂O₇]_∞²⁻ lamellae, the other half Na cations (Na2) distribute in the planes bisecting the [Al₂B₂O₇]_∞²⁻ lamellae. Depending on the composition, the site occupation factor of Na2 site can vary in the same range as x, leading to a tunable density of Na⁺ vacancies in the structure. The AlO₄ tetrahedra and BO₃ triangles in the structure tilt in appropriate ways to improve the bond valence sum of Na2 cations which are not sufficiently bonded to the anions.

Introduction

CaAl₂B₂O₇ was first reported by Schäfer and Kuzel¹ in their study of the ternary system CaO–Al₂O₃–B₂O₃. Two modifications were observed in their investigation: a monoclinic phase believed to be stable at high temperature and a hexagonal phase (*P*6₃22, *a* = 4.81 Å, *c* = 15.55 Å) formed upon prolonged heating at 830 to 900 °C. Later, Chang and Keszler² solved the structure of CaAl₂B₂O₇ in space group *R*3̄*c* (No. 167) with lattice parameters *a* = 4.810(6) Å and *c* = 46.633(5) Å, the latter being about 3 times that of the so-called low-temperature phase. Chang and Keszler also found that a very low level of Na⁺ impurities leads to a completely different powder pattern, which is, interestingly, consistent with the data reported for the low-temperature phase.

Na₂Al₂B₂O₇ crystallizes in space group *P*3̄1*c* (No. 163) with lattice constants *a* = 4.8010(4) Å and *c* = 15.2425(16) Å.³ Both CaAl₂B₂O₇ and Na₂Al₂B₂O₇ consist of [Al₂B₂O₇]_∞²⁻ lamellae stacked along the *c* axis. However, the configuration and the stacking sequence of [Al₂B₂O₇]_∞²⁻ lamellae in these two compounds are different. For details see our recent publication.³

By citing Chang's Ph.D. dissertation, Chang and Keszler² stated that the Na⁺-containing CaAl₂B₂O₇ crystallized in space group *P*6₃22, and the stacking of [Al₂B₂O₇]_∞²⁻ lamellae in this phase was ABAB... rather than ABCABC... as in pure CaAl₂B₂O₇. However, details were not given. We reinvestigated the series Ca_{1-x}Na_{2x}Al₂B₂O₇ and present our results here.

Experimental Section

Sample Preparation. Polycrystalline samples with the composition Ca_{1-x}Na_{2x}Al₂B₂O₇ (x = 0.01, 0.32, 0.90, 0.95, 0.99, and 1.00) were prepared by solid-state reaction using CaCO₃, Na₂CO₃, Al₂O₃, and H₃BO₃ in appropriate ratios as starting materials. The mixtures were first preheated at 500 °C for 20 h, then annealed at 900 °C (for x = 0.01 and 0.32) or 800 °C (for x = 0.90, 0.95, 0.99, and 1.00) for 4 days, and finally cooled to room temperature in the furnace with the power turned off.

Two batches of single crystals were grown. For the first batch, polycrystalline Ca_{0.99}Na_{0.02}Al₂B₂O₇ and NaBO₂ prepared in advance were used as starting materials. The mixture of Ca_{0.99}Na_{0.02}Al₂B₂O₇ and NaBO₂ in a molar ratio 3:2 was melted in a Pt crucible and then allowed to cool slowly. The detailed heating scheme was as follows. The temperature was raised to 1050 °C, held for 5 h, then decreased to 950 °C at a rate of 2 °C/h, then to 800 °C in 50 h, and at last to room temperature in the furnace with the power turned off. For the second batch, polycrystalline Ca_{0.05}Na_{1.90}Al₂B₂O₇ prepared in advance was heated to 1020 °C, held at this temperature for 2 h, then cooled to 950 °C in 50 h, and to 850 °C at a rate of 2 °C/h. Then the power was turned off and the sample was cooled to room temperature in the furnace. Transparent, platelike single

* Author to whom correspondence should be addressed. Fax: +49 711 689 1091. E-mail: m.he@fkf.mpg.de.

(1) Schäfer, V. L.; Kuzel, H. J. *Neues Jahrb. Mineral. Monatsh.* **1967**, 131–136.
(2) Chang, K. S.; Keszler, D. A. *Mater. Res. Bull.* **1998**, 33, 299–304.
(3) He, M.; Kienle, L.; Simon, A.; Chen X. L.; Duppel, V. *J. Solid State Chem.* **2004**, 177, 3212–3218.

Table 1. Crystallographic Data and Details of Structure Determination for $\text{Ca}_{1-x}\text{Na}_x\text{Al}_2\text{B}_2\text{O}_7$ ($x = 0.32$ and 0.95)

formula	$\text{Ca}_{0.69(1)}\text{Na}_{0.64(3)}\text{Al}_2\text{B}_2\text{O}_7$ (1)	$\text{Ca}_{0.05(1)}\text{Na}_{1.90(4)}\text{Al}_2\text{B}_2\text{O}_7$ (2)
M_w (g mol ⁻¹)	230.02	233.26
space group	$P6_3/m$ (No. 176)	$P6_3/m$ (No. 176)
a (Å)	4.8238(5)	4.8138 (7)
c (Å)	15.472(3)	15.301 (3)
V (Å ³)	311.79(7)	307.07 (9)
Z	2	2
D_x (mg m ⁻³)	2.450	2.523
μ (mm ⁻¹)	1.069	0.641
diffractometer	Stoe IPDS II	Stoe IPDS II
radiation	Mo K α	Mo K α
crystal	transparent, platelike	transparent, platelike
crystal size (mm ³)	0.120 × 0.080 × 0.024	0.230 × 0.120 × 0.030
T (K)	293(2)	293(2)
scan type	w	w
absorption correction	numerical	numerical
T_{\min} , T_{\max}	0.8971, 0.9683	0.9162, 0.9819
measured reflns	3735	2154
independent reflns	375	226
reflns with $I > 2\sigma(I)$	347	203
R_{int}	0.0349	0.0610
R_{σ}	0.0164	0.0205
θ_{max}	31.89	26.64
index range	$-6 \leq h \leq 7$, $-7 \leq k \leq 7$, $-23 \leq l \leq 23$	$-6 \leq h \leq 6$, $-5 \leq k \leq 6$, $-16 \leq l \leq 19$
reflns used in refinements	375	226
refined params	29	29
$R[F^2 > 2\sigma(F^2)]$	0.0345	0.0419
$wR(F^2)$	0.0867	0.1125
S	1.095	1.177
weighting scheme	$\omega = 1/[\sigma^2(F_o^2) + (0.0555P)^2 + 0.1724P]$, where $P = (F_o^2 + 2F_c^2)/3$	$\omega = 1/[\sigma^2(F_o^2) + (0.0506P)^2 + 0.7087P]$, where $P = (F_o^2 + 2F_c^2)/3$
$(\Delta/\sigma)_{\text{max}}$	<0.001	<0.001
$\Delta\rho_{\text{max}}$, $\Delta\rho_{\text{min}}$ (eÅ ⁻³)	0.434, -0.508	0.609, -0.318
twin laws	-100, 110, 001	-100, 110, 001
fraction of twin component	0.479(6)	0.48(1)

crystals for X-ray measurement could be easily selected from these two batches of samples. For convenience of description, the crystals of the first and second batch are denoted as crystals **1** and **2**, respectively.

Data Collection and Structure Analysis. Powder diffraction diagrams were recorded using a Stoe Stadi powder diffraction system equipped with an incident beam curved germanium monochromator. Diffraction intensities were collected in Debye–Scherrer geometry with a small linear PSD (2θ range 4°).

Single-crystal diffraction data were collected with a Stoe IPDS system utilizing Imaging Plate detector. Experimental details are listed in Table 1. The program SHELXTL⁴ was used to solve and refine the structure. Neutral atom form factors and anomalous dispersion terms were taken from *International Tables* vol. C.

Results and Discussion

Structure Determination in $P6_322$. The structure determination was first started with the data set collected from crystal **1**. The reflections could be indexed with a hexagonal unit cell, $a = 4.8238(5)$ Å and $c = 15.472(3)$ Å, in good agreement with the previous reports.^{1,2} The absence of reflections $00l$ with $l = 2n + 1$ suggested the possible space groups $P6_3$, $P6_3/m$, and $P6_322$. According to the observed Laue symmetry $6/mmm$ the space group $P6_322$ was selected as the correct one, consistent with the reports in refs 1 and 2. Ca, Al, B, Na, and one O site (at $2d$) could be found without problems via direct methods and subsequent difference Fourier syntheses. All these sites locate on the 3-fold

axis. Two equally significant peaks at general positions ($12i$), which indicate O atoms according to their coordinations to B and Al, were observed in the difference Fourier map. Only one of these can be occupied due to the given stoichiometry. As these two O sites are nearly correlated by a mirror perpendicular to the a or c axis, we supposed an unrecognized merohedral twinning. For the space group $P6_322$, merohedral twinning by a mirror perpendicular to the a or c axis is equal to inversion twinning. However, the refinement with an inversion-twinning model changed the R values only slightly, and the residual peaks in the difference Fourier map were still high. Moreover, the comparison between the one-dimensional projection of the single-crystal data and the simulated pattern of the present structure model showed significant differences with $11l$ reflections for $l = 1, 3, 5, 7, 11$, indicating substantial errors in the structure model, and, possibly, a wrong space group selection.

Structure determination in $P6_3/m$. The Laue group of the other two possible space groups, $P6_3$ and $P6_3/m$, is $6/m$ rather than $6/mmm$, the symmetry observed for diffraction data. However, a merohedral twin with a mirror perpendicular to the a or c axis, and approximately equal volume fractions of the twin components will display a reflection pattern of $6/mmm$ symmetry. Assuming a merohedral twin of $P6_3/m$ individuals, all atoms could be easily located by direct methods and difference Fourier syntheses, and finally residual factors converged to 0.0357 and 0.0925, for $R1$ and $wR2$, respectively.

(4) SHELXTL 6.10; Bruker AXS Inc.: Madison, Wi, 2000.

Table 2. Atomic Coordinates of $Ca_{0.69(1)}Na_{0.64(3)}Al_2B_2O_7$ (1) Obtained at the Early Stage of the Structure Determination

atom	site	sof	x	y	z	U_{eq}^a
Ca/Na1	2b	0.69(1)/0.32(2)	0	0	1/2	0.0124(4)
Na2	2a	0.32(2)	0	0	1/4	0.044(4)
Al	4f	1.0	1/3	2/3	0.35782(6)	0.0098(3)
B	4f	1.0	2/3	1/3	0.4000(2)	0.0119(6)
O1	2c	1	1/3	2/3	1/4	0.060(2)
O2	12i	1	0.4029(4)	0.3697(4)	0.4030(1)	0.0173(4)

$$^a U_{eq} = (1/3)\sum_i \sum_j U_{ij} a_i^* a_j^* a_i a_j$$

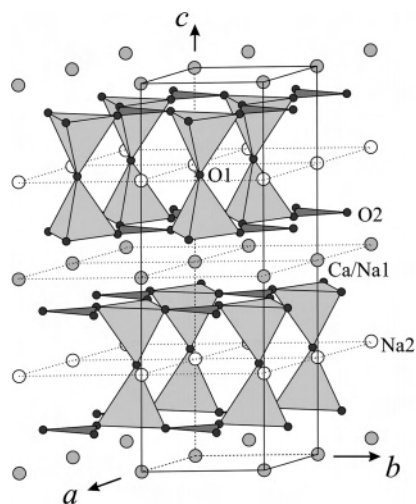


Figure 1. Perspective view of the $Ca_{0.69(1)}Na_{0.64(3)}Al_2B_2O_7$ structure (1). Dark triangles and gray tetrahedra represent BO_3 and AlO_4 groups, respectively.

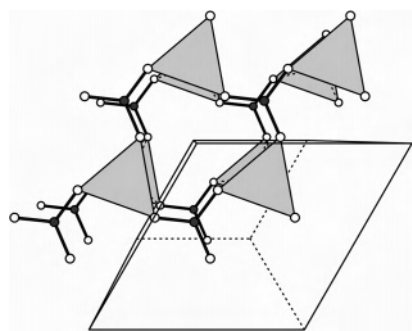


Figure 2. Perspective view of one layer of the $[Al_2B_2O_7]_{\infty}^{2-}$ lamella in the $Ca_{0.69(1)}Na_{0.64(3)}Al_2B_2O_7$ structure (1) along the c axis with the unit cell outlined. Solid circles represent B atoms, open circles represent O atoms, and gray polyhedra represent AlO_4 tetrahedra.

The atomic coordinates obtained at this stage are reported in Table 2. A perspective view of the structure is given in Figure 1. This structure consists of $[Al_2B_2O_7]_{\infty}^{2-}$ lamellae stacked along the c axis and alkaline earth or alkali metal cations distributed between them or in the plane bisecting these lamellae, as found in $CaAl_2B_2O_7$ and $Na_2Al_2B_2O_7$. However, the configuration of the $[Al_2B_2O_7]_{\infty}^{2-}$ lamellae in this structure is different from that of their counterparts in $CaAl_2B_2O_7$ and $Na_2Al_2B_2O_7$ (see Figure 2 and ref 3). The symmetry of the lamellae in this structure belongs to layer group $P6$, while the lamellae in $CaAl_2B_2O_7$ and $Na_2Al_2B_2O_7$ belong to $P321$ and $P312$, respectively. In contrast to the $CaAl_2B_2O_7$ - and $Na_2Al_2B_2O_7$ -type lamellae, the lamella in the present structure is not chiral due to a mirror plane bisecting it. Following the notation system introduced in

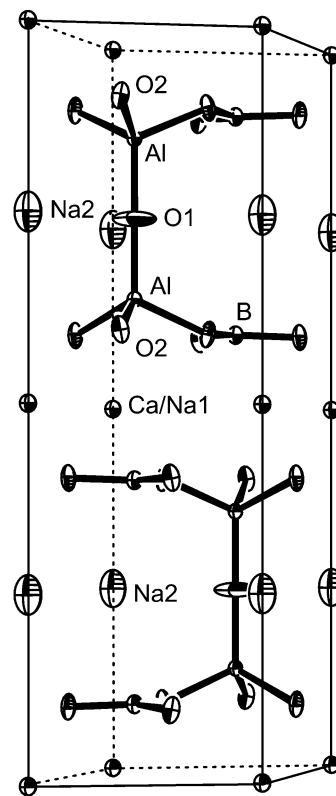


Figure 3. Perspective view of $Ca_{0.69(1)}Na_{0.64(3)}Al_2B_2O_7$ (1) with the displacement ellipsoids drawn at 50% probability.

our previous publication,³ the stacking sequence of the lamellae in the present structure can be described as “...ABAB...” instead of “...A+/B-/A+/B-/...” in $Na_2Al_2B_2O_7$ or “...A+/B-/C+/A-/B+/C-/A+/B-/C+/A-/B+/C-...” in $CaAl_2B_2O_7$.

Ca atoms distribute between these $[Al_2B_2O_7]_{\infty}^{2-}$ lamellae and are coordinated by six O atoms at the vertexes of a trigonal antiprism as found in the structure of $CaAl_2B_2O_7$. In agreement with the findings of Chang and Keszler,² Na^+ can substitute Ca^{2+} according to the formula $Ca_{1-x}Na_{2x}Al_2B_2O_7$. Half of the Na atoms (denoted as Na1) statistically occupy the same crystallographic sites as Ca, and the rest (Na2) locate at the planes bisecting the $[Al_2B_2O_7]_{\infty}^{2-}$ lamellae, i.e., the O1 plane. Again, the coordination of them is quite similar to that found in $Na_2Al_2B_2O_7$.

Without any constraints, the sum of the site occupation factors (sof) of Ca and Na1 refined to 1.01(3), and the composition of the crystal refined to $Ca_{0.69(1)}Na_{0.64(3)}Al_2B_2O_7$, indicating that most Na^+ cations of $NaBO_2$ flux used in the single-crystal growth were incorporated in $Ca_{1-x}Na_{2x}Al_2B_2O_7$.

Although the R -values are quite low, the displacement parameters are suspicious. As can be seen from Figure 3, the displacement amplitudes of Na2 and O1 atoms are much larger than those of other atoms, and, moreover, the displacement ellipsoids of O1 are pancakelike. Actually, the root-mean-squared displacement of O1 in the (001) plane is as large as 0.29 Å, about 3 times that along the [001] direction. Clearly, the large displacement of Na2 correlates with the fact that this atom is not sufficiently bonded to

Table 3. Selected Interatomic Distances (Å) in the Structure of $\text{Ca}_{0.69(1)}\text{Na}_{0.63(3)}\text{Al}_2\text{B}_2\text{O}_7$ (**1**)

Al–O2A	1.793(4)	Ca/Na1–O2A	2.354(5)
Al–O2B	1.733(6)	Ca/Na1–O2B	2.51(1)
Al–O1	1.696(2)		
		Na2–O2A	3.092(9)
		Na2–O2B	2.84(2)
B–O2A	1.379(3)	Na2–O1	2.51(3)
B–O2B	1.371(6)	Na2–O1	2.84(7)
		Na2–O1	3.03(4)

anions, as evidenced by the very low sum of bond valences, 0.438. On the other hand, the large displacement amplitude of O1 in the (001) plane is questionable. When we tried to refine this structure with isotropic O, 3 and 2 strong residual peaks with intensities well above $1.0 \text{ e}\text{\AA}^{-3}$ were observed around O1 and O2, respectively. Accordingly, O1 was moved to the 6 h site, which corresponds to a 3-fold split position around the original site, and O2 was split into two new positions O2A and O2B. Attempts to refine all new O sites anisotropically did not succeed even with restrains because the displacement parameters of O2A and O2B are strongly correlated. Therefore, these two sites are refined isotropically while all other atoms are refined anisotropically. Finally, least-squares calculations converged to slightly lower residual factors, 0.0345 and 0.0867, for $R1$ and $wR2$, respectively. The positional and displacement parameters of all other atoms except for O kept constant within the accuracy. The results of the least-squares refinement are reported in Table 1. Selected interatomic distances are given in Table 3.

Inspection of the split O sites shows that they just represent the tilting of AlO_4 tetrahedra and BO_3 triangles (see Figure 4). Clearly, the insufficiently bonded Na2 is the reason for such tilting. When one Na2 site is occupied, the AlO_4 tetrahedra and BO_3 triangles around it will tilt properly to improve its bond valence sum. For instance, the bond valence sum of Na2 can increase to 0.63 when all the AlO_4 tetrahedra around a Na2 atom tilt in the way shown in Figure 4b. Another reason for the tilting of AlO_4 tetrahedra and BO_3 triangles is the statistical occupation of the same site by Ca and Na1. By tilting the AlO_4 tetrahedra and BO_3 triangles around them in an appropriate way, both can be properly bonded with O. It can be seen from Figure 4b that an AlO_4 tetrahedron will always have two O2 atoms located at O2A sites and one occupying O2B to keep its rigid shape despite the different sites O1 might take. Then the sof of O2A and O2B sites will have to be $2/3$ and $1/3$, respectively, if all AlO_4 tetrahedra in the structure tilt in the way shown in Figure 4. Indeed, the refined sof of O2B is 0.32(4), in good agreement with the prediction, suggesting that all tetrahedra are tilted in this structure. This also agrees with the composition of the crystal.

Structure of Crystal 2. With the structure of crystal **1** as starting model, the refinement on the data set from crystal **2** proceeded well. Its composition refined to $\text{Ca}_{0.05(1)}\text{Na}_{1.90(4)}\text{Al}_2\text{B}_2\text{O}_7$ without any constraints, in perfect agreement with the composition of the starting materials. Crystal data and details of refinement of crystal **2** are reported in Table 1.

It is interesting to note that the AlO_4 tetrahedra in this

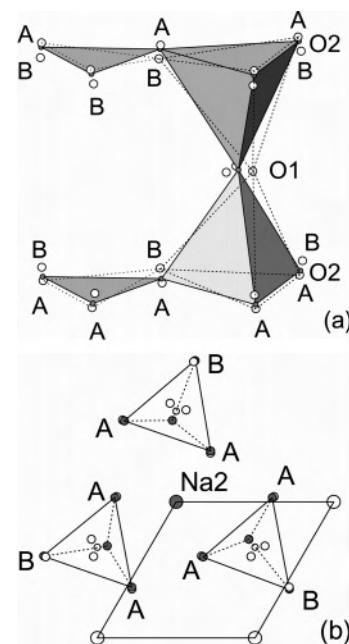


Figure 4. (a) Perspective view and (b) projection along the c axis of a fragment of $[\text{Al}_2\text{B}_2\text{O}_7]_{\infty}^{2-}$ lamella in $\text{Ca}_{0.69(1)}\text{Na}_{0.64(3)}\text{Al}_2\text{B}_2\text{O}_7$ (**1**) with O disorders. In (a), gray tetrahedra and triangles depict untilted AlO_4 and BO_3 groups, respectively. Open circles represent split O positions. Dashed lines show the tilted AlO_4 tetrahedra and BO_3 triangles. In (b) sites occupied are shown as gray circles and labeled while unoccupied sites are not labeled and are characterized with open circles. Dashed lines in (b) represent back edges of AlO_4 tetrahedra. In both (a) and (b), “A” and “B” are used to label O2A and O2B sites, respectively.

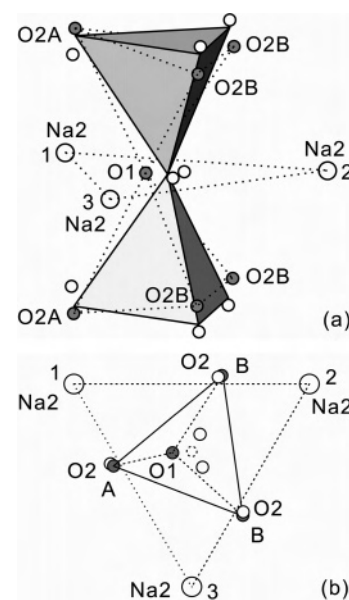


Figure 5. (a) Perspective view and (b) projection along the c axis of a tilted dimer of AlO_4 tetrahedra (Al_2O_7 group) in $\text{Ca}_{0.05(1)}\text{Na}_{1.90(4)}\text{Al}_2\text{B}_2\text{O}_7$ (**2**) and its three closest Na2 neighbors. A dashed small circle in (b) indicates the position of an Al atom. Occupied O sites are highlighted in gray and labeled (for O2) with “A” or “B” to discriminate O2A and O2B sites.

structure tilt in a way different from that in crystal **1**. As can be seen from Figure 5, in this case two O2 atoms of the AlO_4 tetrahedron occupy O2B sites while another one locates at the O2A site no matter which site the O1 atom takes. We name this way of tilting of AlO_4 tetrahedra in crystal **2** as “2B+A”. In contrast, the tilting in crystal **1** is “2A+B”.

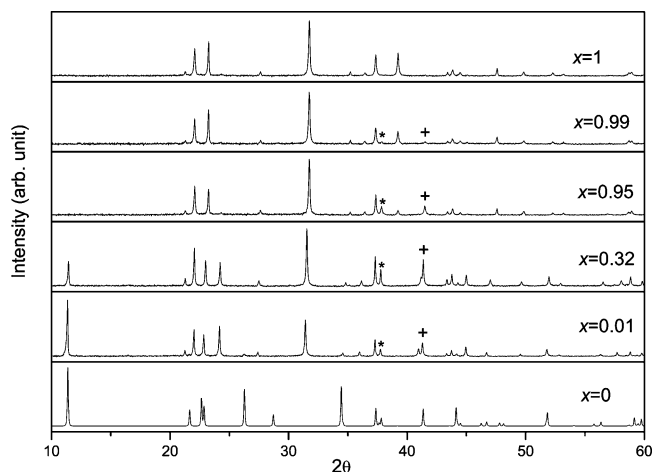


Figure 6. Powder diffraction patterns of Ca_{1-x}Na_{2x}Al₂B₂O₇. Reflections marked with “*” and “+” are 111 and 113, respectively. The pattern for $x = 0$ is simulated with the structure data reported in ref 2 while other patterns are experimental ones (Cu K α 1, 50 s/0.1° in 2θ).

When a dimer of AlO₄ tetrahedra, i.e., Al₂O₇ groups, tilts as shown in Figure 5, its contribution to the bond valence sum of Na₂ atoms at sites 1, 2, and 3 is 0.225, 0.205, and 0.251, respectively, all of which are significantly higher than the value corresponding to the untilted Al₂O₇ dimer, 0.179. On the other hand, the tilted Al₂O₇ dimer in crystal **1** increases its contribution greatly only to one of its closest Na₂ neighbors, while the contribution to the other two Na₂ sites does not improve much or even decreases. In crystal **1**, only 1/3 of the Na₂ sites are occupied, so “2A+B”-type tilting is preferred. In crystal **2**, Na₂ sites are nearly fully occupied, then obviously “2B+A”-type tilting is more appropriate. It has to be mentioned that the refined sof of O2B in crystal **2** is 0.52(3), significantly lower than the expected value of 2/3. The discrepancy has not been understood. Nevertheless, the refined O1 positions agree with the difference Fourier map based on isotropic O atom refinement.

The electron density of the highest residual peak (0.61 eÅ⁻³) is about 2 times that of the second highest one. It corresponds to an O site in the Na₂Al₂B₂O₇-type structure, suggesting that domains of Na₂Al₂B₂O₇-type structure might exist in crystal **2**.

Structure Types and Composition. Several powder diffraction patterns of Ca_{1-x}Na_{2x}Al₂B₂O₇ are shown in Figure 6. By comparison with previously reported data for low- and high-temperature form of CaAl₂B₂O₇, we find that the low-temperature phase is possibly the Na⁺-containing hexagonal phase while the so-called monoclinic high-temperature modification is a mixture of pure trigonal CaAl₂B₂O₇ and Na⁺-containing hexagonal phase. The patterns of the compounds containing both Ca²⁺ and Na⁺ display many common features with that for $x = 1$, but are completely different from that for $x = 0$. Both the configuration of the [Al₂B₂O₇]_∞²⁻ lamellae and their stacking sequence are quite different in the structures of CaAl₂B₂O₇ and compounds containing both Ca²⁺ and Na⁺. On the other hand, the only difference between the trigonal pure Na⁺ phase and the hexagonal compounds containing both Ca²⁺ and Na⁺ is the configuration of the [Al₂B₂O₇]_∞²⁻ lamellae. In both cases, a

[Al₂B₂O₇]_∞²⁻ lamella consists of two layers of AlO₄ tetrahedra and two layers of BO₃ triangles. However, in the hexagonal compounds, layers of AlO₄ tetrahedra and BO₃ triangles in the upper part of a [Al₂B₂O₇]_∞²⁻ lamella are mirror images of their counterparts in the lower part. In the pure Na⁺ phase, every AlO₄ tetrahedron and subsequently BO₃ triangle in the upper part of a [Al₂B₂O₇]_∞²⁻ lamella rotate by a certain angle around the linear O–Al–O bonds relative to their counterparts in the lower part. Thus, the mirror symmetry of the [Al₂B₂O₇]_∞²⁻ lamellae is lost and chirality is gained. If the chirality is not taken into account, the stacking sequence of the [Al₂B₂O₇]_∞²⁻ lamellae is the same in the pure Na⁺ phase and the hexagonal compounds containing both Ca²⁺ and Na⁺.

Although the 111 and 113 reflections have been observed in the powder pattern of the sample with $x = 0.99$ which break the extinction law of $P\bar{3}1c$, the space group of the pure Na⁺ phase, it is difficult to distinguish between the pure hexagonal phase (space group $P6_3/m$) or a mixture of hexagonal and trigonal (space group $P\bar{3}1c$) phases. Moreover, it is possible that the range of homogeneity also depends on the heat treatment of the sample. According to our preparation and single crystal analysis, the hexagonal phase could be obtained by cooling the sample slowly in the furnace over a range of composition from $x = 0.01$ to $x = 0.95$. The trigonal phases are obtained only at the very extreme part of the Ca_{1-x}Na_{2x}Al₂B₂O₇ series. Accordingly, the density of Na⁺ vacancies in this structure can be tuned in a very large range by modifying the ratio of Ca²⁺ and Na⁺ in the starting materials.

In the structures of the trigonal pure Na⁺ phase and the hexagonal compounds containing both Ca²⁺ and Na⁺, the distribution of Na⁺ and O²⁻ in the plane bisecting the [Al₂B₂O₇]_∞²⁻ lamellae is reminiscent of the conduction plane of Na⁺ β -alumina.⁵ In the hexagonal compounds, the number of sites available for Na⁺ can by far exceed the number of actual Na⁺ cations and, hence, significant ionic conductivity can be expected for the hexagonal phases.

A close inspection of the powder diagrams reveals a high-angle shift of diffraction peaks with increasing x in the range $0.01 \leq x \leq 0.95$. The decrease of the unit cell size is also confirmed by our X-ray single-crystal measurements. In the series Ca_{1-x}Na_{2x}Al₂B₂O₇ ($0.01 \leq x \leq 0.95$), one Ca²⁺ is replaced by two Na⁺ cations with increasing x , and Na⁺ is larger than Ca²⁺ (for coordination number = 6), so it is surprising to find that the unit cell is getting smaller with x . The explanation can be that with increasing x more and more Na₂ sites are occupied in the structure, which is contracted in order to improve their bond valence sums.

Remarks on SrAl₂B₂O₇. MacDowell⁶ observed two modifications of SrAl₂B₂O₇, cubic and hexagonal, in 1990. Later, SrAl₂B₂O₇ was suggested as a nonlinear optical material together with Na₂Al₂B₂O₇ and the complete solid solubility between them was reported.⁷ However, further

(5) Edström, K.; Thomas, J. O.; Farrington, G. C. *Acta Crystallogr. B* **1991**, *47*, 210–216.

(6) MacDowell, J. F. *J. Am. Ceram. Soc.* **1990**, *73*, 2287–2292.

(7) Keszler, D. A. *Curr. Opin. Solid State Mater. Sci.* **1999**, *4*, 155–162.

work on these compounds showed that $\text{SrAl}_2\text{B}_2\text{O}_7$ is isostructural with $\text{CaAl}_2\text{B}_2\text{O}_7$,⁸ and $\text{Na}_2\text{Al}_2\text{B}_2\text{O}_7$ crystallizes in another centrosymmetric space group $P\bar{3}1c$.³ Considering these reports and our findings in the $\text{Ca}_{1-x}\text{Na}_{2x}\text{Al}_2\text{B}_2\text{O}_7$ system, one expects similarity of the $\text{Sr}_{1-x}\text{Na}_{2x}\text{Al}_2\text{B}_2\text{O}_7$ system.

(8) Lucas, F.; Jaulmes, S.; Quarton, M.; Le Mercier, T.; Guillen F.; Fouassier, C. *J. Solid State Chem.* **2000**, *150*, 404–409.

Acknowledgment. We thank Ms. C. Kamella for her help in preparing the figures. This work is financially supported by the Max Planck Society.

Supporting Information Available: Crystallographic data in CIF format. This material is available free of charge via the Internet at <http://pubs.acs.org>.

IC0500863